CRYSTAL GROWTH & DESIGN

Article

Ce(III)-based Frameworks: From 1D Chain to 3D Porous Metal-Organic Framework

Parviz Gohari Derakhshandeh, Sara Abednatanzi, Karen Leus, Jan Janczak, Rik Van Deun, Pascal Van Der Voort, and Kristof Van Hecke

Cryst. Growth Des., **Just Accepted Manuscript** • DOI: 10.1021/acs.cgd.9b00949 • Publication Date (Web): 24 Oct 2019

is published by the American Chemical Society. 1155 Sixteenth Street N.W., Washington, DC 20036

Ce(III)-based Frameworks: From 1D Chain to 3D Porous Metal-Organic Framework

Parviz Gohari Derakhshandeh[*a,b†], Sara Abednatanzi[a†], Karen Leus[a] , Jan Janczak[c], Rik Van Deun[d], Pascal Van Der Voort[a], Kristof Van Hecke[*b]

[a] COMOC, Department of Chemistry, Center for Ordered Materials, Organometallics and Catalysis, Ghent University, Krijgslaan 281 – Building S3, B-9000 Ghent, Belgium

[b] XStruct, Department of Chemistry, Ghent University, Krijgslaan 281 – Building S3, B-9000 Ghent, Belgium

[c] Institute of Low Temperature and Structure Research, Polish Academy of Sciences, P.O. Box 1410, 50-950 Wroclaw, Poland

[d] L^3 – Luminescent Lanthanide Lab, Department of Chemistry, Ghent University, Krijgslaan 281 – Building S3, B-9000 Ghent, Belgium

† Both authors contributed equally to this work

ABSTRACT

The reaction of pyridine-2,4-dicarboxylic acid (H_2pydc) with $Ce(NO_3)_3.6H_2O$, by applying only minor changes to the reaction conditions, generated a series of new one-, two-, and three-dimensional coordination polymers namely, $[Ce(pydc)(Hpydc)(H_2O)_4]_n$ (**1**), $[Ce(pydc)(Hpydc)(H_2O)_2]_n$ (**2**), and $\{[Ce_3(pydc)_4(H_2O)_2NO_3].4H_2O\}_n$ (**3**). The ancillary ligand interaction as well as the reaction conditions determine the specific coordination modes for the $Hpydc^-$ and $pydc^{2-}$ ligands and, in turn, discriminate between 1D, 2D, and 3D frameworks. Characterization of the prepared materials was performed using single-crystal and powder X-ray diffraction analysis, Fourier transform infrared, CHN elemental analysis, thermogravimetric analysis and nitrogen adsorption/desorption techniques. Compound **1** consists of 1D chains, that

compose of Ce^{3+} ions bridged by $Hpydc^-$ and $pydc^{2-}$ ligands, which further link via non-covalent interactions to form a 3D supramolecular architecture. Compound **2** assembles into 2D sheets with 1D channels. Similarly, via hydrogen bonding interactions between two adjacent sheets, the 2D layers are further stacked into the final 3D supramolecular structure. Compound **3** is a 3D metal-organic framework (MOF), showing 1D helical channels. The progressive skeletal variation from the 1D chains (**1**) to 2D sheets (**2**) and 3D framework (**3**) is attributed to the flexibility of both the Ce(III) coordination sphere and coordination modes of the $Hpydc^-$ and $pydc^{2-}$ ligands under different reaction conditions. The three compounds illustrate how the tuning of the coordination geometry of Ce(III) translates into different dimensionality, which is readily influenced by reaction temperature and ancillary ligand presence. Moreover, the porosity of MOF **3** was confirmed by N_2 and CO_2 gas adsorption/desorption. Finally, the catalytic activity of MOF **3** was examined in acetalization reactions in a series of aromatic aldehydes with methanol.

INTRODUCTION

Metal-organic frameworks (MOFs) are a class of porous materials constructed from inorganic metal nodes, connected via/through multidentate organic bridging ligands. These nanoporous solids have received tremendous attention because of their large specific surface area and especially their structural variety, making them outstanding candidates to be used for various applications such as catalysis[1-3], gas storage[4-5], magnetism[6-7], sensing[8-10] and drug delivery[11].

Within this context, the design of coordination polymers (CPs) and MOFs have gained widespread interest during the last decades due to the vast diversity of organic ligands and metal nodes that can be incorporated in such compounds to construct intriguing architectures and topologies. Numerous attempts have been geared for the design of CPs and MOFs, using the local geometry of metal ions and functional ligands. Nevertheless, it is still challenging to control the dimensionality of the target compounds, structural topology and pore dimensions to obtain advanced MOF materials, suitable for more specialized applications[12-15].

Lanthanide (Ln) CPs have attracted current research efforts due to their high and significant flexibility in coordination modes and numbers, as they can incorporate various modular and adjustable multi-dimensional framework materials[16-22]. The combination of lanthanide luminescence, magnetic, and Lewis acid properties, with the diversity and features of CPs, can potentially be applied in heterogeneous catalysis[23-25], luminescent molecular thermometers[26-28], sensors[29-32], and magnetic compounds[33]. The coordination modes in transition metals are mostly controlled by d-orbital directional features. In contrast, due to the shielded valence orbitals in lanthanide ions, they do not display specific coordination geometries and show significant flexibility in both coordination numbers and geometries. Therefore, design and control over the coordination sphere of lanthanide frameworks appears to be challenging, due to the effect of several factors, such as metal-ligand interactions, auxiliary ligand nature, outer-sphere counter ion, hydrogen bonding groups and reaction conditions (temperature, solvent, pH, etc.). So far, very few studies have reported the rational design and synthesis of rare earth CPs and MOFs. The report of Ayhan et al. described the structural coordination chemistry of two new Ce(III)-based MOFs. In this case, small changes to the reaction conditions resulted in distinctive structures[34]. Another study demonstrated the formation of tubular Ln-based formworks depending on the reaction conditions as well as the counterion. In the presence of Cl^- or NO_3^- anions, a tubular structure was formed, while by using BF_4^- and OAc^- anions, a zigzag 2D compound was obtained[35].

Since Ln coordination compounds display significant flexibility in both coordination numbers and geometries, we targeted Ce(III)-based frameworks as promising candidates for designing new structures[36-37]. The large ionic radius of Ce(III) ions allows to adjust coordination modes by adapting reaction conditions to produce distinctive structures. In this work, we report the design and synthesis of three new Ce(III)-based frameworks using 2,4-pyridinedicarboxylic acid as a linker. Small changes to the reaction conditions led to three different structures ranging from a one-dimensional coordination polymer to a three-dimensional porous MOF. Moreover, the catalytic properties of 3D MOF in acetalization reactions of different aldehydes with methanol were investigated.

EXPERIMENTAL SECTION

Materials and General Methods. All chemicals were purchased from commercial sources and used without further purification. Chemical bonding was analyzed by infrared spectroscopy, using a Thermo Scientific FT-IR spectrometer (type Nicolet 6700) equipped with a DRIFTS-cell. Samples were prepared by mixing the powders with KBr. The samples were measured in the 550-4000 cm^{-1} range. Thermogravimetric analysis (TGA) and Differential Thermal Analysis (DTA) were performed with a Shimadzu TGA-51 and a DTA-50 apparatus under flowing air at 50 mL min^{-1} and a heating rate of 10 ºC min^{-1}. Nitrogen sorption studies were performed at -196 °C using a Belsorp-mini II gas analyzer. Before the adsorption experiments, the sample was degassed under vacuum at 120 °C for 24 h. XRD patterns were recorded on a Thermo Scientific ARLX'TRA diffractometer equipped with a Cu Kα (λ = 1.5405 Å) source, a goniometer and a Peltier cooled Si (Li) solid state detector. In order to determine the conversion of the products, an ultra-fast GC equipped with a flame ionization detector (FID) and a 5% diphenyl/95% polydimethylsiloxane column with 10 m length and 0.10 mm internal diameter was applied. Helium was used as the carrier gas and the flow rate was programmed to be 0.8 mL min^{-1}. The reaction products were recognized using a TRACE GC × GC (Thermo, Interscience) coupled to a TEMPUS TOFMS detector (Thermo, Interscience). The first column consists of a dimethyl polysiloxane
package and has a length of 50 m with an internal diameter of 0.25 mm, whereas the second column has a length of 2 m with an internal diameter of 0.15 mm. The package of the latter is 50% phenyl polysilphenylene-siloxane.

X-ray Crystallography. For the structures of **1** and **2**, X-ray intensity data were collected at 100 K, on a Rigaku Oxford Diffraction Supernova Dual Source (Cu at zero) diffractometer equipped with an Atlas CCD detector using ω scans and CuKα (λ = 1.54184 Å) or MoKα (λ = 0.71073 Å) radiation, for **1** and **2**, respectively. For the structure of **3**, graphite monochromatic Mo-Kα radiation (λ = 0.71073 Å) on a four-circle κ geometry KUMA KM-4 diffractometer, with a two-dimensional area CCD detector, was used. The images were interpreted and integrated with the program CrysAlisPro[38]. Using Olex2[39], the structures were solved by direct methods using the SHELXT program and refined by full-matrix least-squares on F^2 using the SHELXL program

package[40-41]. Non-hydrogen atoms were anisotropically refined and the hydrogen atoms in the riding mode and isotropic temperature factors fixed at 1.2 times U(eq) of the parent atoms. Hydroxyl H-atoms were located when possible through a Fourier difference electron density map (refined with isotropic temperature factors fixed at 1.5 times U(eq)). In crystal **3** it was possible to localize and refine some of the disordered solvent/water molecules. The rest of the solvent molecules (nicotinamide) are highly disordered. The correct modelling of the disordered molecules was not possible and we performed a "squeeze" treatment to remove the scattering contribution of these molecules, which could not to be satisfactory modelled. In total, 61 electrons were removed from solvent accessible voids in a P1 unit cell. As one nicotinamide molecule equals 64 electrons, it's most likely that one nicotinamide molecule is disordered, or (as Z = 4), there's an extra of 1/4th of a nicotinamide molecule per formula unit ($C_{28}H_{24}Ce_3N_5O_{25}$).

The final difference Fourier maps showed no peaks of chemical significance. CCDC 1897917-1897919 contain the supplementary crystallographic data for this paper and can be obtained free of charge via www.ccdc.cam.ac.uk/conts/retrieving.html (or from the Cambridge Crystallographic Data Centre, 12, Union Road, Cambridge CB2 1EZ, UK; fax: +44-1223-336033; or deposit@ccdc.cam.ac.uk).

Synthesis. *[Ce(pydc)(Hpydc)(H_2O)$_4$]$_n$ (**1**).* A mixture of $Ce(NO_3)_3 \cdot 6H_2O$ (0.218 g, 0.5 mmol) and 2,4-H_2pydc (0.126 g, 0.75 mmol) was refluxed for 1 h in 5 mL of water. The resulting solution was filtered and left to stand at room temperature. Pale-yellow single crystals, suitable for X-ray crystallography, were obtained by slow evaporation after five weeks (yield 63%). Elemental Anal. Calcd for $C_{14}H_{15}CeN_2O_{12}$: C, 30.94; H, 2.78; N, 5.15%. Found: C, 31.51; H, 3.34; N, 4.87%. IR (cm^{-1}): 3249 br/m, 1677 w, 1587 s, 1548 m, 1479 w, 1440 w, 1392 m, 1371 s, 1280 m, 1093 w, 1012 w, 777 m.

*[Ce(pydc)(Hpydc)(H_2O)$_2$]$_n$ (**2**).* A mixture of $Ce(NO_3)_3 \cdot 6H_2O$ (0.218 g, 0.5 mmol) and 2,4-H_2pydc (0.126 g, 0.75 mmol) in 3 mL of H_2O was placed in a 12 mL Teflon-lined stainless steel autoclave. The mixture was heated to 100 °C within 15 min, then kept at this temperature for 1 h and cooled to ambient temperature within 24 h. Light-yellow crystals of **2** were filtered off, washed with water and dried in air (yield 60%). Elemental Anal. Calcd for $C_{14}H_{11}CeN_2O_{10}$: C, 33.11; H, 2.18; N, 5.51%. Found: C, 32.89; H, 2.16; N, 5.11%. IR (cm^{-1}): 3326 br/m, 3120 br, 1693 m, 1666 w, 1604

s, 1562 m, 1471 m, 1427 m, 1371 m, 1276 m, 1249m, 1191 w, 1093 w, 1006 w, 939 w, 875 w, 771 s, 707 s.

*{[$Ce_3(pydc)_4(H_2O)_2NO_3$].4H_2O 0.25$C_6H_6N_2O$}$_n$ (**3**).* A mixture of $Ce(NO_3)_3 \cdot 6H_2O$ (0.218 g, 0.5 mmol), 2,4-H_2pydc (0.126 g, 0.75 mmol) and nicotinamide (0.062 g, 0.5 mmol) in 3 mL of H_2O was placed in a 12 mL Teflon-lined stainless steel autoclave. The mixture was heated to 100 °C within 15 min, then kept at this temperature for 1 h and cooled to ambient temperature within 24 h. Yellow crystals of **3** were filtered off, washed with water and dried in air (yield 51%). Elemental Anal. Calcd for $C_{29.5}H_{25.5}Ce_3N_{5.5}O_{25.25}$: C, 27.60; H, 2.00; N, 6.00%. Found: C, 30.31; H, 2.30; N, 5.35% (an extra of 1/4th of a nicotinamide molecule was taken into account in the elemental analysis, according to the X-ray analysis) IR (cm^{-1}): 3305 br/m, 1645 s, 1592 vs, 1481 s, 1454 s, 1402 vs, 1305 w, 1245 w, 1095 w, 1014 m, 883 w, 831 w, 788s, 725s.

In addition, compound **3** can also be obtained by performing the reaction at 150 °C instead of 100 °C and without the addition of nicotinamide, however in this case the crystals were not suitable for the X-ray single crystal analysis.

General procedure for the acetalization reaction of benzaldehyde. During a typical catalytic test, MOF **3** (0.008mmol, 10 mg), dodecane as an internal standard (0.2 mmol), benzaldehyde (0.33 mmol) and methanol (0.5 ml) were added into a Schlenk tube. The tube was sealed and then heated to 40 °C for 24 h. After each catalytic run, the catalyst was recovered by filtration, washed with methanol and used directly in the subsequent runs. Samples were withdrawn after 24 h reaction, and after cooling and dilution with the solvent, were analyzed using an ultra-fast gas chromatograph (Thermo, Interscience) equipped with a flame ionization detector (FID).

RESULTS AND DISCUSSION

Synthesis and Preliminary Characterization. CP **1**, $[Ce(pydc)(Hpydc)(H_2O)_4]_n$, was synthesized by conventional heating of $Ce(NO_3)_3 \cdot 6H_2O$ and 2,4-H_2pydc in a molar ratio of 2:3 in water at 100 °C. After slow evaporation within 5 weeks, pale-yellow single crystals of **1** were obtained. In addition, a yellow precipitation of **1** can be obtained in a shorter time by refluxing a more concentrated solution for 3 h in water. CP **2**, $[Ce(pydc)(Hpydc)(H_2O)_2]_n$, was synthesized

with the same reaction mixture as **1** but using a hydrothermal condition at 100 °C. After cooling of the mixture during 24 h to room temperature, light-yellow crystals of **2** were prepared. MOF **3**, $\{[Ce_3(pydc)_4(H_2O)_2NO_3].4H_2O\}_n$, was synthesized under the same conditions as **2**. However, nicotinamide was added as an ancillary ligand, which gives the yellow suitable for the X-ray analysis single crystals of **3**. Although the nicotinamide ligand is not coordinated in the product, its presence is crucial for the growth of the crystalline 3D MOF **3**, since without it the 2D CP **2** is obtained. The presence of trace amounts of disordered nicotinamide in **3** was confirmed during the refinement of the crystal structure, as well as by observing some discrepancy between calculated and experimental results of elemental analysis. All of the prepared compounds are stable in air.

The IR spectra of all compounds show characteristic strong and broad bands for the coordinated carboxylate groups (COO^-) of the 2,4-pydc ligands in the ranges of 1587-1604 cm^{-1} and 1371-1402 cm^{-1}, for the asymmetric and symmetric stretching vibrations, respectively. In addition, the characteristic broad peaks of the O-H vibration of water and/or carboxylic acid groups centered at around 3241 cm^{-1} (**1**), 3318 (**2**) cm^{-1} and 3305 cm^{-1} (**3**) (Figure S1).

The thermal stability of **1**, **2** and **3** was determined by means of thermogravimetric analysis (TGA). The CP **1** is stable up to 148 °C and then starts to completely decompose till 722 °C with a mass loss of 63.18% (calc. 67.7%). The exothermic peak at 473-548 °C in the DTA curve shows that compound **1** is fully decomposed. CP **2** reveals three mass loss steps after 172.6 °C. The coordination framework is thermally stable up to 397 °C and at higher temperature, with an exothermic peak at 397-522 °C, the decomposition appears with a mass loss of 63.3% (calc. 66.0%). The TGA profile for MOF **3** shows a first weight loss step of 11.8% up to 148.8 °C, which is probably attributed to the loss of four water molecules and a nitrate anion (calc. 10.7%). The second mass loss of 2.8% occurs at 224 °C which may be due to the loss of two coordinated water molecules (calc. 2.9%). On further heating, the decomposition of the organic components in **3** are observed, showing an exothermic peak at 393-498 °C (Figure S2).

The experimental powder XRD patterns for compounds **1**, **2** and **3** are in good agreement with the corresponding simulated ones (Figure S3).

Structural Analysis. The reactions of the 2,4-H_2pydc ligand with $Ce(NO_3)_3.6H_2O$ led to the formation of three 1D, 2D and 3D coordination frameworks. The structures of these compounds

were characterized by single-crystal X-ray diffraction. The crystallographic data and structure refinement parameters for all materials are summarized in Table 1. The corresponding bond lengths and angles in the coordination sphere of the Ce(III) cations are listed in Table S1. The coordination modes of the pydc ligand in compounds **1**, **2** and **3** are presented in scheme 1.

Table 1. Crystal data and refinement details for **1**, **2** and **3**

Empirical formula	$C_{14}H_{15}CeN_2O_{12}$ (**1**)	$C_{14}H_{11}CeN_2O_{10}$ (**2**)	$C_{28}H_{24}Ce_3N_5O_{25}$ (**3**)
Formula weight	543.40	507.37	1250.88
Temperature	100.0 K	100.0 K	100.0 K
Wavelength	1.5418 Å	0.71073 Å	0.71073 Å
Crystal system	triclinic	triclinic	tetragonal
Space group	*P*-1	*P*-1	$P4_32_12$
Unit cell dimensions	a = 6.3729(4) Å	a = 6.2373(2) Å	a = 9.6303(6) Å
	b = 6.6115(2) Å	b = 9.3746(5) Å	b = 9.6303(6) Å
	c = 19.9859(6) Å	c = 14.2072(5) Å	c = 52.293(3) Å
	α = 82.857(3)°	α = 72.685(4)°	α = 90°
	β = 81.281(4)°	β = 84.587(3)°	β = 90°
	γ = 81.673(4)°	γ =71.604(4)°	γ = 90°
Volume	819.06(6) Å^3	752.55(6) Å^3	4849.8(7) Å^3
Z	2	2	4
Density (calculated)	2.203 Mg/m^3	2.239 Mg/m^3	1.697 Mg/m^3
Absorption coefficient	22.211 mm^{-1}	3.091 mm^{-1}	2.894 mm^{-1}
F(000)	534.0	494.0	2356
Crystal size	0.18 x 0.07 x 0.068 mm^3	0.294 x 0.147 x 0.089 mm^3	0.17 x 0.18 x 0.19 mm^3
Theta range for data collection	9.00 to 150.706°	4.77 to 59.36°	2.4 to 29.5°
Index ranges	$-7\leq h \leq 7$	$-8\leq h \leq 8$	$-12\leq h \leq 13$
	$-8\leq k \leq 7$	$-12\leq k \leq 12$	$-12\leq k \leq 12$
	$-22\leq l \leq 25$	$-18\leq l \leq 19$	$-69\leq l \leq 66$
Reflections collected	10829	16655	52792
Independent reflections	3285 [R(int) = 0.0632]	3837 [R(int) = 0.0818]	6251 [R(int) = 0.050]
Absorption correction	Numerical	Numerical	Numerical
Refinement method	Full-matrix least-squares on F^2	Full-matrix least-squares on F^2	Full-matrix least-squares on F^2
Data / restraints / parameters	3285 / 13 / 289	3837 / 6 / 257	6251 / 0 / 272
Goodness-of-fit on F^2	1.042	1.044	1.006
Final *R*. [I>2sigma(I)]	R_1 = 0.0422, wR_2 = 0.1088	R_1 = 0.0383, wR_2 = 0.0681	R_1 = 0.0478, wR_2 = 0.1142
***R* indices (all data)**	R_1 = 0.0445, wR_2 = 0.1114	R_1 = 0.0509, wR_2 = 0.0735	R_1 = 0.0520, wR_2 = 0.1164
Flack parameter	-	-	-0.014(15)

Largest diff. peak, hole	1.41 and -1.35 e.Å^{-3}	1.08 and -1.19 e.Å^{-3}	1.75 and -1.57 e.Å^{-3}

*Crystal structure of **1***. CP **1** crystallizes in the triclinic centrosymmetric space group *P*-1. The asymmetric unit of **1** contains one Ce(III) cation coordinated by one pydc^{2-} and one Hpydc^{-} anionic ligands and four coordinated water molecules. The central Ce(III) ion is nine-coordinated to eight oxygen atoms, from four water molecules, four carboxylate groups, and one nitrogen atom of a pydc^{2-} ligand (Figure 1a). In **1**, two Ce(III) centers are connected via two pydc^{2-} ligands to produce a binuclear unit. These units are connected to each other by carboxylic groups to make a one-dimensional channel (Figure 1b and 1c). In fact, each pydc^{2-} ligand acts as a tetradentate bridging ligand and is coordinated to one Ce(III) in a bidentate fashion through the pyridine nitrogen atom and a carboxylate oxygen atom and two more Ce(III) ions in a monodentate fashion through single carboxylate oxygen atoms. Furthermore, a Hpydc^{-} ligand is bound to each Ce(III) center through a single carboxylate oxygen atom. As shown in scheme 1a and 1b, in compound **1** two different coordination modes of pydc are observed, which are coordinated to 1 and 3 distinct Ce(III) ions, respectively. Extensive non-covalent interactions such as π···π stacking interactions and strong O−H···O hydrogen bonds exist between two neighboring chains. The π···π stacking interactions (with centroid-centroid distances of 3.712 Å) between single 1D chains, as illustrated in Figure 1d, plays an important role in the final framework. Furthermore, the coordinated water molecules contribute to the formation of intermolecular hydrogen bonds involving carboxylate O atoms (Table S2). As a result, the 1D chains are further assembled into a 3D supramolecular network (Figure 1d and 1e). To describe the 1D architecture of **1** more clearly, the TOPOS program[42] was used to analyze the topological structure. If every Ce ion is regarded as a node and each Hpydc^{-} and pydc^{2-} ligands serves as a linker, CP **1** could simplify as a 3-c net (uninodal net) topological structure, characterized by $\{4^2.6\}$ point symbol (Figure 4a).

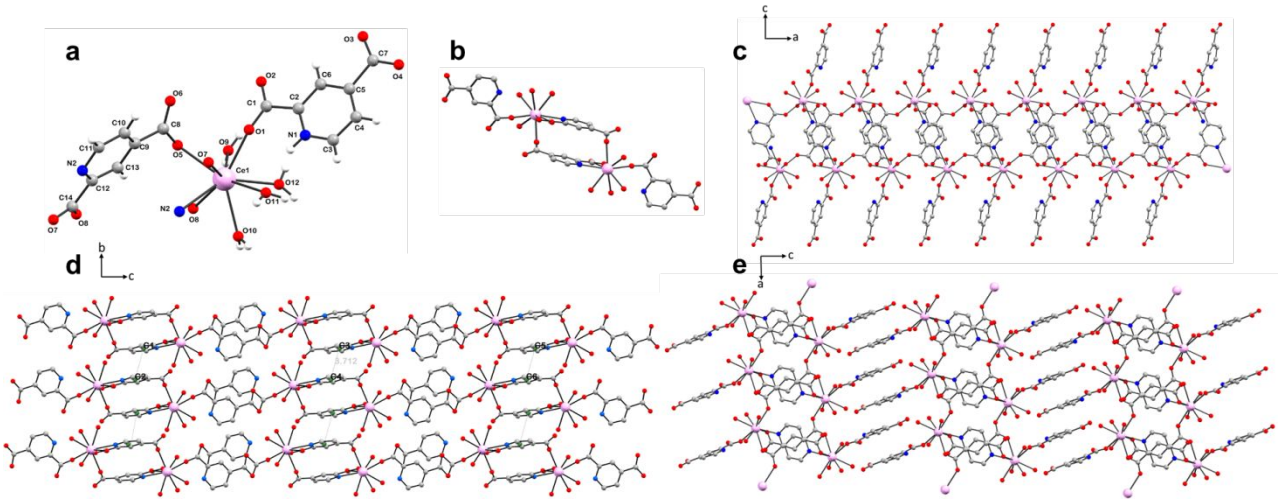

Figure 1. (a) Coordination environment of the Ce(III) cation in **1**. (b, c) Fragment of the 1D coordination polymer chain of **1**. (d, e) Fragment of the 3D supramolecular framework of **1.**

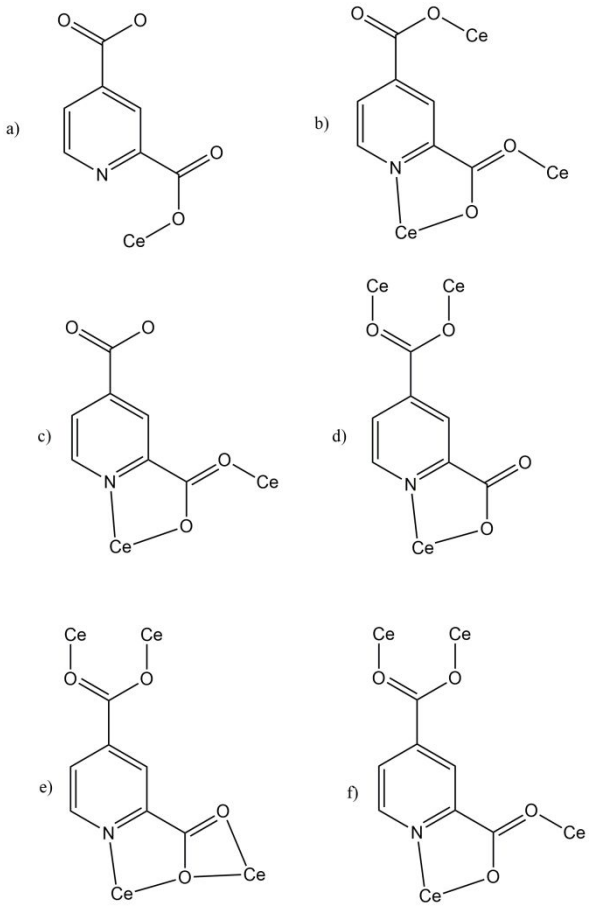

Scheme 1. The coordination modes of the 2,4-pydc ligands in the (a, b) structure **1**, (c,d) structure **2** and (e,f) structure **3**.

*Crystal structure of **2***. CP **2** crystallizes in the triclinic centrosymmetric space group *P*-1 and the asymmetric unit consists of a Ce(III) cation, one $pydc^{2-}$ and one $Hpydc^{-}$ ligands and two coordinated water molecules. Here, the Hpydc- ligand has a protonated carboxyl group instead of a protonated pyridine nitrogen atom. The Ce(III) center is coordinated to five $pydc^{2-}$ units and two water molecules to form an overall nine-coordinated local geometry of the metal center (Figure 2a). Three $pydc^{2-}$ units are monodentately coordinated to the Ce(III) center through a single carboxylate atom and two remaining $pydc^{2-}$ units are coordinated in a bidentate fashion, similar to the one seen in CP **1**, through a carboxylate oxygen atom and a pyridine nitrogen atom. As indicated in scheme 1c and 1d in compound **2** also two different coordination modes of $pydc^{2-}$ are observed, which are coordinated to 2 and 3 distinct Ce(III) ions, respectively. Finally, two water molecules are bound to complete the nine-coordination of the Ce(III). Viewing down the a-axis reveals that the Ce(III) metal ions are linked via a carboxylate group, from one of the $pydc^{2-}$ linkages. Furthermore, another carboxylate group is bridging the Ce(III) ions to complete the overall 2D structure (Figure 2b-2d). Similar to the CP **1,** extensive face-to-face π···π stacking interactions of pyridyl rings with centroid-centroid distances of 3.937 Å exist between the neighboring layers. In addition, strong O−H···O hydrogen bonds of the coordinated water molecules and protonated carboxylate O atoms in collaboration with π···π stacking serves to connect 2D sheets of **2** into a 3D supramolecular framework (Figure 2e-f). Corresponding hydrogen bonding distances and angles are listed in Table S2. For better insight into this intricate net of the 2D coordinating polymer, a topological analysis of compound **2** was performed. It's structure consists of layers parallel to (001) with a thickness of 9.22 Å and can also be simplified to simple node-and-linker net using topology approach. The CP **2** structure could simplify as a 3,5-c net with stoichiometry (3-c)(5-c); 2-nodal net characterized by $\{4^2.6^7.8\}\{4^2.6\}$ point symbol (Figure 4b).

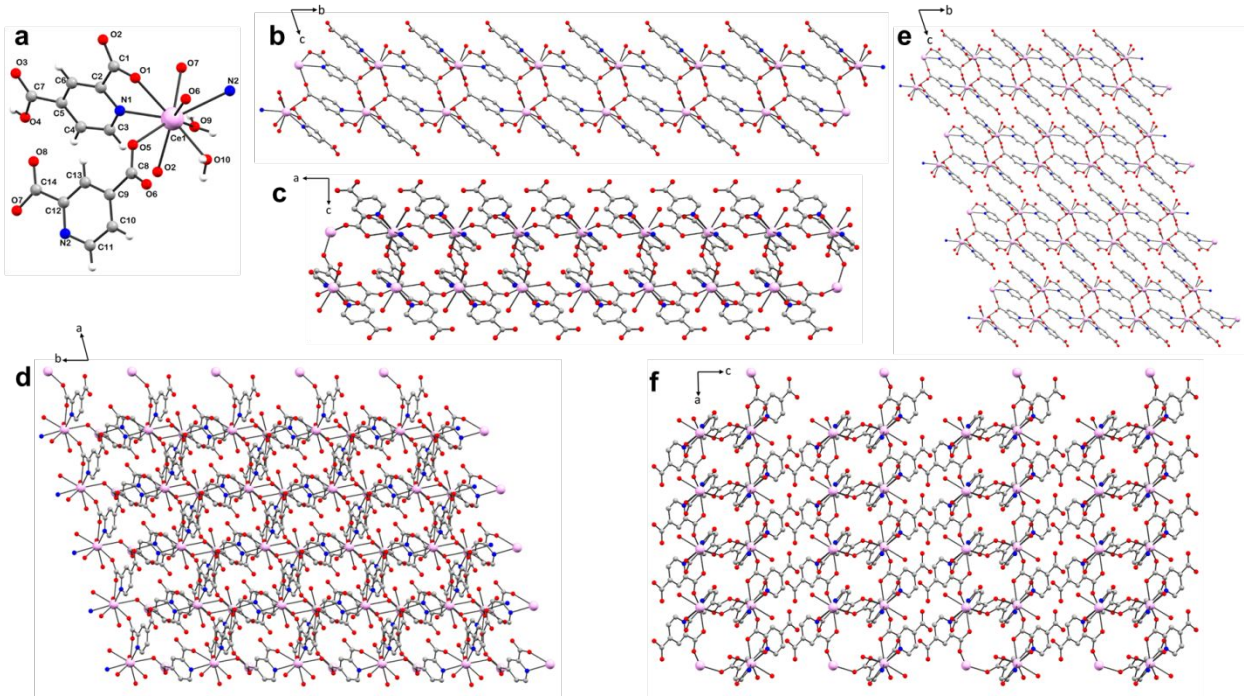

Figure 2. (a) Coordination environment of the Ce(III) cation in **2**. (b, c and d) Fragment of the 2D coordination polymer grid of **2**. (e, f) Fragment of the 3D supramolecular framework of **2.**

Crystal structure of 3. MOF **3** crystallizes in the tetragonal non-centrosymmetric space group $P4_32_12$ and the asymmetric unit contains two crystallographically independent Ce1 and Ce2 centers, two pydc^{2-} ligands, one and half of coordinated water, one half of coordinated nitrate ion and four halves of non-coordinated water molecules that are disordered (Figure 3a). The Ce2 center is found on a special position (2-fold axis), while the nitrate anion is observed in half occupancy. In **3**, the Ce1 is eight-coordinated whereas the Ce2 is nine-coordinated similar to those in **1** and **2**. The Ce1 coordinates to five pydc^{2-} ligands and statistically to one nitrate anion or water molecule to form the overall 8-coordinate local geometry of the metal center. Three pydc^{2-} units are bound to the Ce(III) ion though a single carboxylate oxygen atom. The two other pydc^{2-} ligands are bound to the Ce1 center in a bidentate mode via a carboxylate oxygen atom and pyridine nitrogen atom. A nitrate anion or a water molecule (both with the occupation factor of 0.5) is bound to complete the coordination sphere of the Ce1 (CeO_6N_2) (See Figure 3b). The Ce2 coordinates to four pydc^{2-} in a monodentate fashion through a single oxygen atom of carboxylate groups and two other pydc^{2-} in a bidentate mode via their carboxylate groups. Finally, one oxygen atom of a water molecule is

coordinated to complete the nine-coordination of the Ce2 (CeO_9) (Figure 3b). As it can be seen in scheme 1e and 1f, in compound **3** again two different coordination modes of $pydc^{2-}$ are observed, which are coordinated to 4 and 4 separate Ce(III) ions respectively. Viewing down the b-axis shows that the Ce1 and Ce2 centers are connected through bridging carboxylate groups to form the overall 3D network consisting of a helical channel with diagonal distance of 9.630 × 9.630 $Å^2$ determined via the Ce ions distance (Figure 3c-d). Disordered water molecules as solvent molecules that have been localized, as well as disordered nicotinamide molecules, highly disordered, which have not been modeled, fill the channels in the structure. Note that due to the wavelike structure, the channels are not elongated. The porosity of MOF **3** was confirmed by N_2 adsorption isotherm. In order to better identify the intricate net of the 3D MOF, suitable connectors can be defined by using topological approach. As exhibited in Figure 4c Ce ion (pink) is regarded as a node and each $pydc^{2-}$ ligand serves as a linker, MOF **3** could simplify as a 8-c net (uninodal net) characterized by $\{3^6.4^{16}.5^6\}$ point symbol.

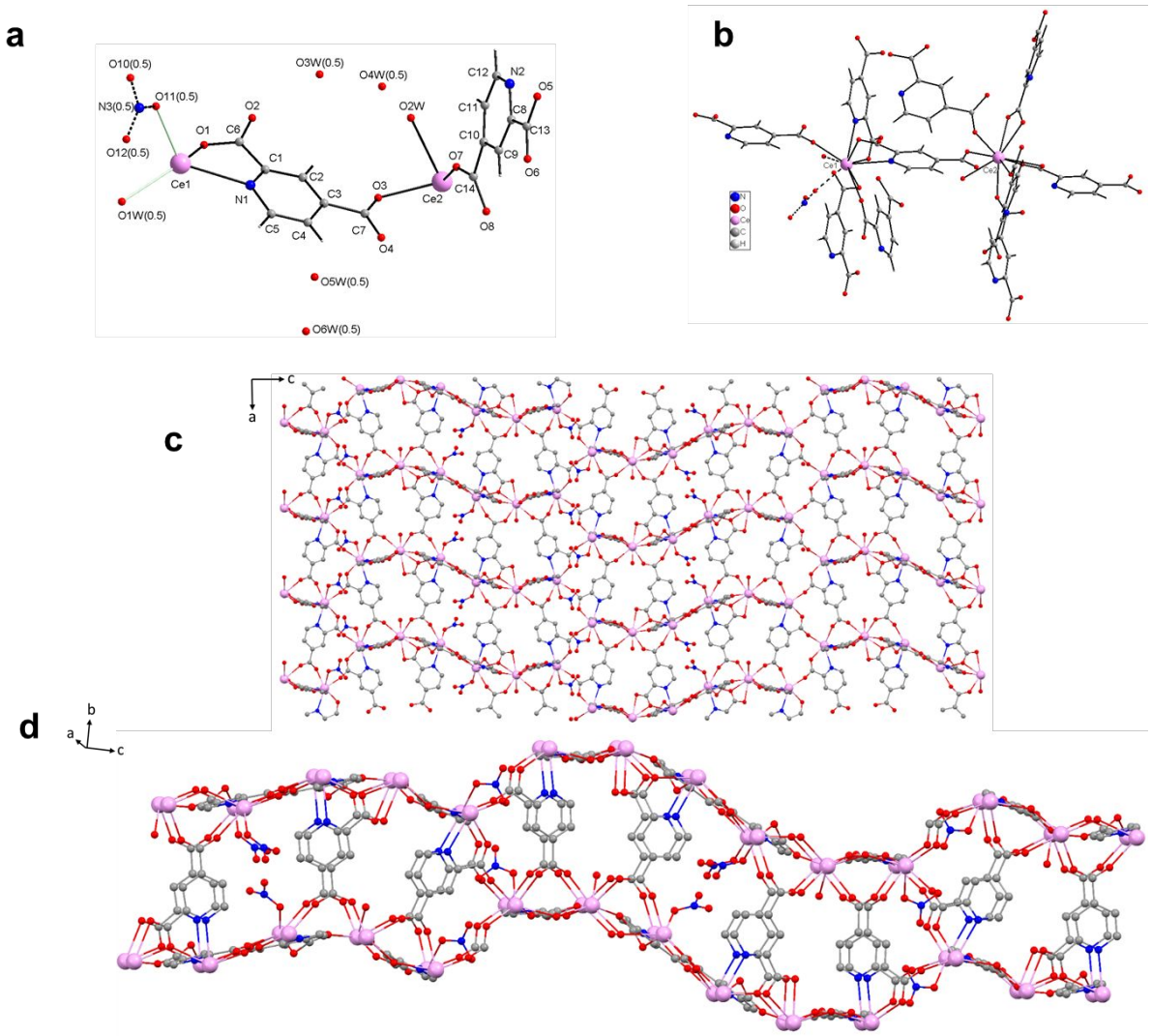

Figure 3. (a) Asymmetric unit of **3**. (b) Coordination environment of Ce1 and Ce2. (c) Fragment of the 3D network of 3. (d) View of helical channel in **3**.

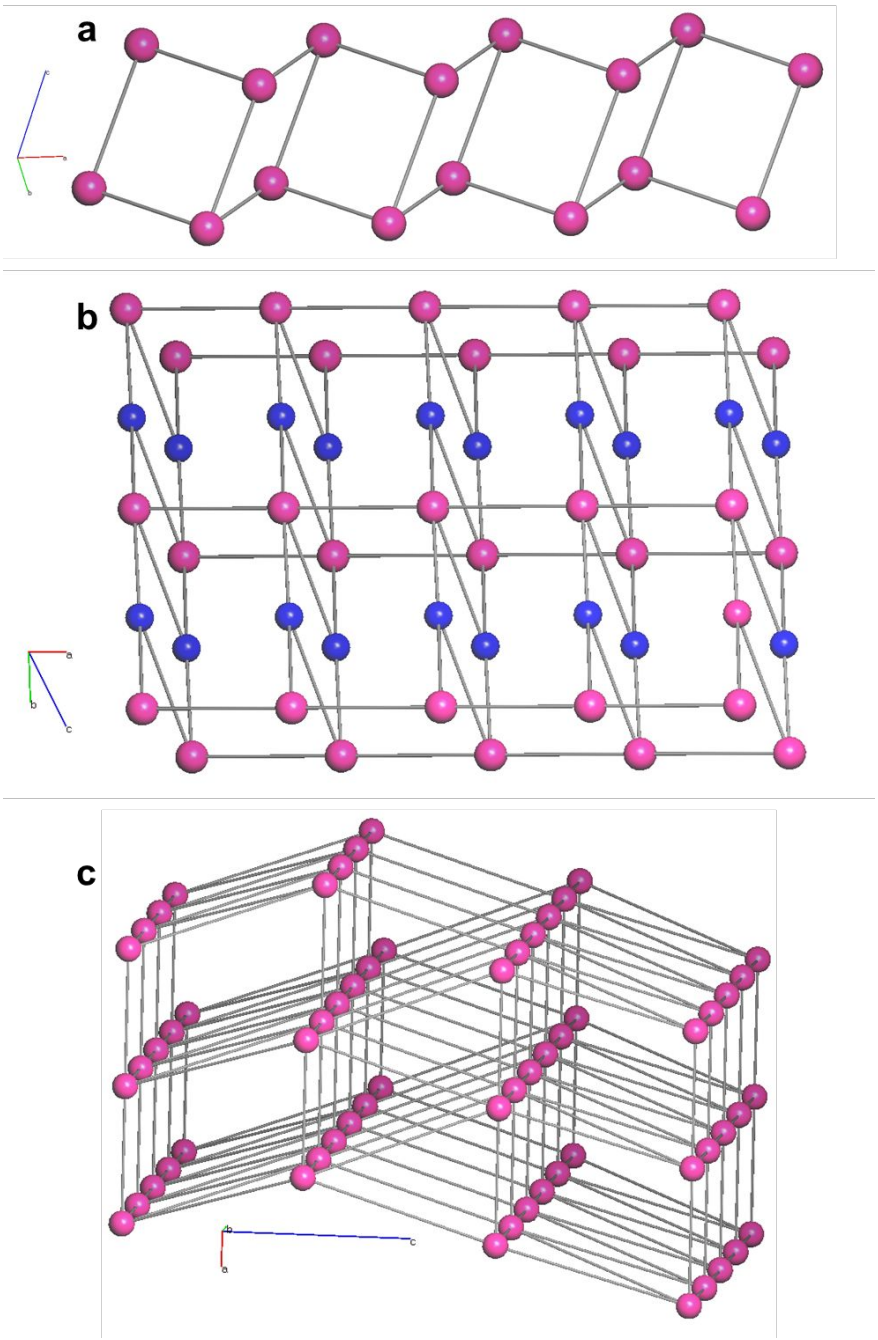

Figure 4. View of (a) the 3-c net topological structure of **1**, (b) the 3,5-c net with stoichiometry (3-c)(5-c) of **2** (color codes: blue codes represent the center ring of the 3-connected $Hpydc^-$ and $pydc^{2-}$ ligands and pink codes represent Ce^{3+} ions) and (c) the `8-c net` topological structure of **3**.

The adsorption characteristics of the frameworks in MOF **3** was investigated, and its porosity was confirmed by the N_2 and CO_2 adsorption isotherms at 77 and 298 K, respectively. As demonstrated

in Figure 5, after desolvation the framework maintains a permanent porosity and exhibits a Langmuir surface area (S_{lang}) of 310 m^2 g^{-1} with a pore volume of 0.15 cm^3 g^{-1}. Gas adsorption measurement at 1 bar was performed to investigate the CO_2 uptake capacities of **3**, which is shown in Figure S4 in Supporting Information. After activation at 120 °C under vacuum overnight, the adsorption capacities of MOF **3** for CO_2 was 0.81 mmol g^{-1} at room temperature.

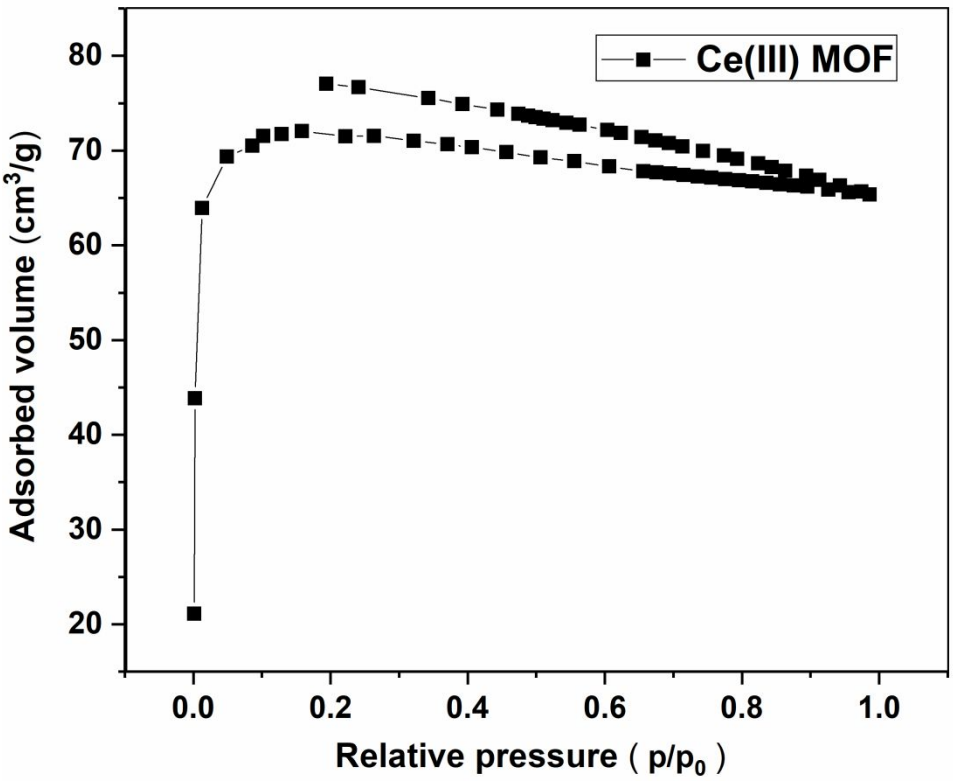

Figure 5. Nitrogen sorption isotherm of MOF **3**.

The 1D Compound **1** is formed by refluxing the reaction mixture, while the same reaction mixture under hydrothermal condition resulted in the 2D structure **2**. This may be due to the higher reaction temperature in the closed system which plausibly leads to various coordination modes of the pydc ligand. Furthermore by adding the nicotinamide to the identical reaction mixture under the same conditions as material **2** the 3D compound **3** is obtained. Although the nicotinamide ligand does not coordinate to the Ce centers, it can facilitate the coordination of pydc to the metal centers through deprotonating 2,4-H_2pydc and also via non-covalent interactions. From these observations it can be concluded that the applied reaction conditions have a direct impact on the obtained

structures. Furthermore, an ancillary ligand can conduct the obtained product to a specific structure even without being in the final framework.

So far there are a few reported lanthanide-based coordination polymers using 2,4-H_2pydc as the ligand[43-46]. However, these structures are bimetallic or oxalate was used as the ancillary ligand. To the best of our knowledge, the only Ce-based coordination polymer with 2,4-H_2pydc ligand is reported by Lush et. al.[47] In this compound, the Ce(III) cation is nine-coordinated ($CeNO_8$) and formed by three pydc anions, one oxalate anion, and three water molecules. The oxalate and pydc ligands bridge the Ce(III) cations, forming a two-dimensional coordination polymer. The $pydc^{2-}$ ligand acts as a tetradentate bridging ligand similar the coordination mode observed in our 1D coordination polymer (scheme 1b) and is coordinated to one Ce(III) in a bidentate fashion through the pyridine nitrogen atom and a carboxylate oxygen atom and two more Ce(III) ions in a monodentate fashion through single carboxylate oxygen atoms.

Catalytic acetalization reaction. Lewis acid metal sites are known to promote the acetalization reaction of aldehydes.[48-50] Therefore, the catalytic activity of MOF **3** was investigated for the acetalization reaction of benzaldehyde and methanol as model reactants. The obtained results are given in Table 2. In the presence of benzaldehyde and methanol as the substrates and MOF **3** catalyst, a good conversion of 80% with 99% selectivity towards benzaldehyde dimethyl acetal as the desired product was observed. In order to clarify the general applicability of the MOF **3** catalyst, various substrates and different alcohols such as ethanol, ethylene glycol and 1,3-propanediol were tested and the obtained results are listed in Table 2. In general, the catalyst showed a good activity for all types of examined substrates as well as complete selectivity towards the correspondent product. Additionally, the catalytic activity of compound **1** (1D) and compound **2** (2D) were investigated for the acetalization reaction of benzaldehyde and methanol under the same reaction conditions. The catalysts showed good catalytic activity with conversions of 82 and 83% respectively (Table 2, entry 2 and 3).

Based on the work of Kanai and coworker[51] the possible reaction mechanism is illustrated in Figure S7. As shown, the removal of water molecules of the framework creates open coordination sites capable of attaching to organic molecules. Hereafter, the interaction of both benzaldehyde and methanol with the Ce center and coordinated oxygens can facilitate the nucleophilic addition of the OH group in methanol on the carbon atom of the aldehyde group in benzaldehyde to give the

hemiacetal derivative analogous. Afterward, the hemiacetal reacts with another methanol molecule, most likely with the assistance of the Ce-MOF catalyst, to give the corresponding acetal derivative.

The recyclability of MOF **3** was examined after separation of the catalyst from reaction mixture at the end of the reaction. The recovered catalyst was reused at least 3 times for the acetalization reaction of benzaldehyde with methanol and the obtained results are given in Figure S5. As can be observed, the recovered MOF **3** maintains similar activity after 3 recycles. Further evidence of the stability of the catalyst was confirmed by PXRD analysis after 3 times reuse (Figure S6).

Table 2. Catalytic performance of the MOF **3** catalyst towards the acetalization reaction of various benzaldehyde derivatives with alcohols.

Entry	Benzaldehyde derivatives	Alcohol	Product
1	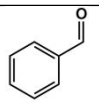	CH_3OH	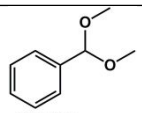 79 (99%)
2[a]	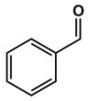	CH_3OH	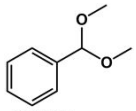 82 (99%)
3[b]	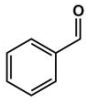	CH_3OH	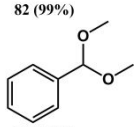 83 (99%)
4[c]	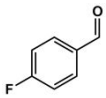	CH_3OH	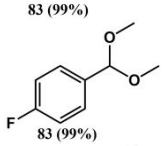 83 (99%)
5[c]	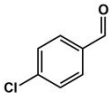	CH_3OH	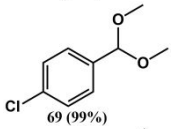 69 (99%)
6[c]	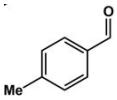	CH_3OH	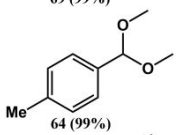 64 (99%)
7[c]	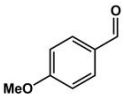	CH_3OH	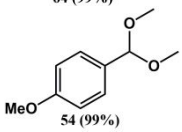 54 (99%)

8[d]	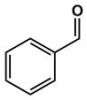	CH_3CH_2OH	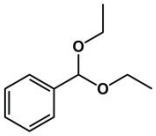 54 (99%)
9[e]	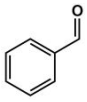		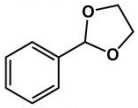 87 (78%)
10[f]	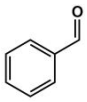	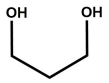	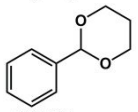 98 (99%)

Reaction conditions: 0.33 mmol benzaldehyde, 0.008 mmol catalyst (10 mg), 0.5 ml methanol, 0.2 mmol dodecane, 40 °C, 24 h, Conversions are determined based on GC-MS. Selectivity is towards the related acetal. Conversion and selectivity are reported respectively in parenthesis. [a] Compound 1 (1D) was used as the catalyst (0.008 mmol, 4.3 mg). [b] Compound 2 (2D) was used as the catalyst (0.008 mmol, 4 mg). [c] 60 °C. [d] Ethanol, [e] Ethylene glycol and [f] 1,3-Propanediol were used as the solvent, respectively.

CONCLUSION

In summary, we have developed three new 1D, 2D and 3D Ce(III)-based frameworks by small changes in the synthetic routs. The obtained results revealed the importance of the reaction conditions as well as the ancillary ligand for the preparation of distinctive structures and the effect on the properties of the materials. This shows that the lanthanide ions do not have the preference for a specific coordination geometry because of their valence orbitals which are buried inside. Therefore the nature of coordination modes in lanthanide ions is controlled by a subtle interplay between metal-ligand and interligand steric interactions depending on the reaction conditions. These findings demonstrate that Ce(III) ions are outstanding candidates to adopt distinct coordination environments due to their adjustable coordination modes which is an important step towards the design of Ce(III)-based frameworks for more specialized applications. The MOF **3** showed good activity and selectivity in acetalization reaction and could be recycled without loss of activity or selectivity.

Supporting Information

Selected bond lengths [Å] and angles [°] for **1**, **2** and **3**, Hydrogen bonds geometry, catalyst characterizations including DRIFT spectra, TGA, XRD, CO_2 sorption, recycling studies, proposed reaction mechanism and GC-MS spectra. Tables S1-S2 and Figures S1-S7.

Acknowledgements

The authors thank the University of Gent for all the supports. PGD and SA gratefully acknowledges the financial support from the Research Foundation Flanders (FWO-Vlaanderen) grant No. G000117N. SA acknowledges the financial support from the Ghent University BOF doctoral grant 01D04318. KVH thanks the Special Research Fund (BOF) – UGent (project 01N03217) for funding. RVD thanks the Hercules Foundation (project AUGE/09/024 "Advanced Luminescence Setup") for funding. KVH and RVD thank the Hercules Foundation (project AUGE/11/029 "3D-SPACE: 3D Structural Platform Aiming for Chemical Excellence") for funding.

References

1. Abednatanzi, S.; Leus, K.; Derakhshandeh, P. G.; Nahra, F.; De Keukeleere, K.; Van Hecke, K.; Van Driessche, I.; Abbasi, A.; Nolan, S. P.; Van Der Voort, P., POM@IL-MOFs - inclusion of POMs in ionic liquid modified MOFs to produce recyclable oxidation catalysts. *Catal Sci Technol* **2017**, *7*, 1478-1487.
2. Abednatanzi, S.; Derakhshandeh, P. G.; Abbasi, A.; Van der Voort, P.; Leus, K., Direct Synthesis of an Iridium(III) Bipyridine Metal-Organic Framework as a Heterogeneous Catalyst for Aerobic Alcohol Oxidation. *Chemcatchem* **2016**, *8*, 3672-3679.
3. Huang, Y. B.; Liang, J.; Wang, X. S.; Cao, R., Multifunctional metal-organic framework catalysts: synergistic catalysis and tandem reactions. *Chem Soc Rev* **2017**, *46*, 126-157.
4. Wang, H. H.; Shi, W. J.; Hou, L.; Li, G. P.; Zhu, Z. H.; Wang, Y. Y., A Cationic MOF with High Uptake and Selectivity for CO2 due to Multiple CO2-Philic Sites. *Chem-Eur J* **2015**, *21*, 16525-16531.
5. Zhang, Y. B.; Furukawa, H.; Ko, N.; Nie, W. X.; Park, H. J.; Okajima, S.; Cordova, K. E.; Deng, H. X.; Kim, J.; Yaghi, O. M.,

Introduction of Functionality, Selection of Topology, and Enhancement of Gas Adsorption in Multivariate Metal Organic Framework-177. *J Am Chem Soc* **2015**, *137*, 2641-2650.
6. Chuang, Y. C.; Ho, W. L.; Sheu, C. F.; Lee, G. H.; Wang, Y., Crystal engineering from a 1D chain to a 3D coordination polymer accompanied by a dramatic change in magnetic properties. *Chem Commun* **2012**, *48*, 10769-10771.
7. Bauer, W.; Schlamp, S.; Weber, B., A ladder type iron(II) coordination polymer with cooperative spin transition. *Chem Commun* **2012**, *48*, 10222-10224.
8. Mukherjee, S.; Desai, A. V.; More, Y. D.; Inamdar, A. I.; Ghosh, S. K., A Bifunctional Metal-Organic Framework: Striking CO2-Selective Sorption Features along with Guest-Induced Tuning of Luminescence. *Chempluschem* **2016**, *81*, 702-707.
9. Pal, S.; Bharadwaj, P. K., A Luminescent Terbium MOF Containing Hydroxyl Groups Exhibits Selective Sensing of Nitroaromatic Compounds and Fe(III) Ions. *Cryst Growth Des* **2016**, *16*, 5852-5858.
10. Gao, R. C.; Guo, F. S.; Bai, N. N.; Wu, Y. L.; Yang, F.; Liang, J. Y.; Li, Z. J.; Wang, Y. Y., Two 3D Isostructural Ln(III)-MOFs: Displaying the Slow Magnetic Relaxation and Luminescence Properties in Detection of Nitrobenzene and Cr2O72-. *Inorg Chem* **2016**, *55*, 11323-11330.
11. An, J. Y.; Geib, S. J.; Rosi, N. L., Cation-Triggered Drug Release from a Porous Zinc-Adeninate Metal-Organic Framework. *J Am Chem Soc* **2009**, *131*, 8376-+.
12. Zhang, J. P.; Zhang, Y. B.; Lin, J. B.; Chen, X. M., Metal Azolate Frameworks: From Crystal Engineering to Functional Materials. *Chem Rev* **2012**, *112*, 1001-1033.
13. Kitagawa, S.; Kitaura, R.; Noro, S., Functional porous coordination polymers. *Angew Chem Int Edit* **2004**, *43*, 2334-2375.
14. Yaghi, O. M.; O'Keeffe, M.; Ockwig, N. W.; Chae, H. K.; Eddaoudi, M.; Kim, J., Reticular synthesis and the design of new materials. *Nature* **2003**, *423*, 705-714.
15. Furukawa, H.; Cordova, K. E.; O'Keeffe, M.; Yaghi, O. M., The Chemistry and Applications of Metal-Organic Frameworks. *Science* **2013**, *341*, 974-+.
16. Cui, Y. J.; Yue, Y. F.; Qian, G. D.; Chen, B. L., Luminescent Functional Metal-Organic Frameworks. *Chem Rev* **2012**, *112*, 1126-1162.
17. Duan, J. G.; Higuchi, M.; Foo, M. L.; Horike, S.; Rao, K. P.; Kitagawa, S., A Family of Rare Earth Porous Coordination Polymers with Different Flexibility for CO2/C2H4 and CO2/C2H6 Separation. *Inorg Chem* **2013**, *52*, 8244-8249.
18. Guo, H. L.; Zhu, Y. Z.; Qiu, S. L.; Lercher, J. A.; Zhang, H. J., Coordination Modulation Induced Synthesis of Nanoscale Eu(1-

x)Tb(x-)Metal-Organic Frameworks for Luminescent Thin Films. *Adv Mater* **2010**, *22*, 4190-+.
19. Le Natur, F.; Calvez, G.; Daiguebonne, C.; Guillou, O.; Bernot, K.; Ledoux, J.; Le Polles, L.; Roiland, C., Coordination Polymers Based on Heterohexanuclear Rare Earth Complexes: Toward Independent Luminescence Brightness and Color Tuning. *Inorg Chem* **2013**, *52*, 6720-6730.
20. Freslon, S.; Luo, Y.; Calvez, G.; Daiguebonne, C.; Guillou, O.; Bernot, K.; Michel, V.; Fan, X., Influence of Photoinduced Electron Transfer on Lanthanide-Based Coordination Polymer Luminescence: A Comparison between Two Pseudoisoreticular Molecular Networks. *Inorg Chem* **2014**, *53*, 1217-1228.
21. Derakhshandeh, P. G.; Soleimannejad, J.; Janczak, J., Sonochemical synthesis of a new nano-sized cerium(III) coordination polymer and its conversion to nanoceria. *Ultrason Sonochem* **2015**, *26*, 273-280.
22. Derakhshandeh, P. G.; Soleimannejad, J.; Janczak, J.; Kaczmarek, A. M.; Van Hecke, K.; Van Deun, R., Mechanochemically synthesized crystalline luminescent 2D coordination polymers of La3+ and Ce3+, doped with Sm3+, Eu3+, Tb3+, and Dy3+: synthesis, crystal structures and luminescence. *Crystengcomm* **2016**, *18*, 6738-6747.
23. Xiong, Y. H.; Chen, S. H.; Ye, F. G.; Su, L. J.; Zhang, C.; Shen, S. F.; Zhao, S. L., Synthesis of a mixed valence state Ce-MOF as an oxidase mimetic for the colorimetric detection of biothiols. *Chem Commun* **2015**, *51*, 4635-4638.
24. Ji, P. F.; Sawano, T.; Lin, Z. K.; Urban, A.; Boures, D.; Lin, W. B., Cerium-Hydride Secondary Building Units in a Porous Metal-Organic Framework for Catalytic Hydroboration and Hydrophosphination. *J Am Chem Soc* **2016**, *138*, 14860-14863.
25. Lin, A.; Ibrahim, A. A.; Arab, P.; El-Kaderi, H. M.; El-Shall, M. S., Palladium Nanoparticles Supported on Ce-Metal-Organic Framework for Efficient CO Oxidation and Low-Temperature CO2 Capture. *Acs Appl Mater Inter* **2017**, *9*, 17961-17968.
26. Kaczmarek, A. M.; Liu, Y. Y.; Wang, C.; Laforce, B.; Vincze, L.; Van Der Voort, P.; Van Hecke, K.; Van Deun, R., Lanthanide "Chameleon" Multistage Anti-Counterfeit Materials. *Adv Funct Mater* **2017**, *27*, 1700258.
27. Rao, X. T.; Song, T.; Gao, J. K.; Cui, Y. J.; Yang, Y.; Wu, C. D.; Chen, B. L.; Qian, G. D., A Highly Sensitive Mixed Lanthanide Metal-Organic Framework Self-Calibrated Luminescent Thermometer. *J Am Chem Soc* **2013**, *135*, 15559-15564.
28. Cui, Y. J.; Xu, H.; Yue, Y. F.; Guo, Z. Y.; Yu, J. C.; Chen, Z. X.; Gao, J. K.; Yang, Y.; Qian, G. D.; Chen, B. L., A Luminescent Mixed-Lanthanide Metal-Organic Framework Thermometer. *J Am Chem Soc* **2012**, *134*, 3979-3982.

29. Hu, Z. C.; Deibert, B. J.; Li, J., Luminescent metal-organic frameworks for chemical sensing and explosive detection. *Chem Soc Rev* **2014**, *43*, 5815-5840.
30. Meyer, L. V.; Schonfeld, F.; Muller-Buschbaum, K., Lanthanide based tuning of luminescence in MOFs and dense frameworks - from mono- and multimetal systems to sensors and films. *Chem Commun* **2014**, *50*, 8093-8108.
31. Tan, H. L.; Liu, B. X.; Chen, Y., Lanthanide Coordination Polymer Nanoparticles for Sensing of Mercury(II) by Photoinduced Electron Transfer. *Acs Nano* **2012**, *6*, 10505-10511.
32. Xu, H.; Hu, H. C.; Cao, C. S.; Zhao, B., Lanthanide Organic Framework as a Regenerable Luminescent Probe for Fe3+. *Inorg Chem* **2015**, *54*, 4585-4587.
33. Malaestean, I. L.; Kutluca-Alici, M.; Ellern, A.; van Leusen, J.; Schilder, H.; Speldrich, M.; Baca, S. G.; Kogerler, P., Linear, Zigzag, and Helical Cerium(III) Coordination Polymers. *Cryst Growth Des* **2012**, *12*, 1593-1602.
34. Ayhan, O.; Malaestean, I. L.; Ellern, A.; van Leusen, J.; Baca, S. G.; Kogerler, P., Assembly of Cerium(III) 2,2 '-Bipyridine-5,5 '-dicarboxylate-based Metal-Organic Frameworks by Solvent Tuning. *Cryst Growth Des* **2014**, *14*, 3541-3548.
35. Ghosh, S. K.; Bharadwaj, P. K., Coordination polymers of La(III) as bunched infinite nanotubes and their conversion into an open-framework structure. *Inorg Chem* **2005**, *44*, 3156-3161.
36. Ebrahim, A. M.; Bandosz, T. J., Ce(III) Doped Zr-Based MOFs as Excellent NO2 Adsorbents at Ambient Conditions. *Acs Appl Mater Inter* **2013**, *5*, 10565-10573.
37. Lammert, M.; Glissmann, C.; Reinsch, H.; Stock, N., Synthesis and Characterization of New Ce(IV)-MOFs Exhibiting Various Framework Topologies. *Cryst Growth Des* **2017**, *17*, 1125-1131.
38. Buettner, G. R., Spin Trapping - Electron-Spin-Resonance Parameters of Spin Adducts. *Free Radical Bio Med* **1987**, *3*, 259-303.
39. Dolomanov, O. V.; Bourhis, L. J.; Gildea, R. J.; Howard, J. A. K.; Puschmann, H., OLEX2: a complete structure solution, refinement and analysis program. *J Appl Crystallogr* **2009**, *42*, 339-341.
40. Sheldrick, G. M., A short history of SHELX. *Acta Crystallogr A* **2008**, *64*, 112-122.
41. Sheldrick, G. M., Crystal structure refinement with SHELXL. *Acta Crystallogr C* **2015**, *71*, 3-8.
42. Blatov, V. A.; Shevchenko, A. P.; Proserpio, D. M., Applied Topological Analysis of Crystal Structures with the Program Package ToposPro. *Cryst Growth Des* **2014**, *14*, 3576-3586.
43. Huang, Y. G.; Wu, M. Y.; Wei, W.; Gao, Q.; Yuan, D. Q.; Jiang, F. L.; Hong, M. C., Unprecedented ferromagnetic interaction in an erbium(III)-copper(II) coordination polymer. *J Mol Struct* **2008**, *885*, 23-27.

44. Min, D.; Lee, S. W., Terbium-oxalate-pyridinedicarboxylate coordination polymers suggesting the reductive coupling of carbon dioxide (Co-2) to oxolate (C2O42-): [Tb-2 (3,5-PDC)(2)(H2O)(4)(C2O4)]center dot 2H(2)O and [Tb(2,4-PDC) (H2O) (C2O4)(0.5)] (PDC = pyridinedicarboxylate). *Inorg Chem Commun* **2002**, *5*, 978-983.
45. An, X. P.; Wang, H. S.; Li, G. C., Structures and Luminescent Properties of Two 2D Coordination Polymers Containing Tb(III) or Dy(III) Ions. *J Fluoresc* **2014**, *24*, 425-429.
46. Lush, S. F.; Shen, F. M., Poly[hexaaquahexakis(mu-pyridine-2,4-dicarboxylato)tricopper(II)-dieuropium(III)]. *Acta Crystallogr E* **2010**, *66*, M1516-U370.
47. Shen, F. M.; Lush, S. F., Poly[[hexaaqua(mu(2)-oxalato-kappa O-4(1),O-2:O-1 ',O-2 ')bis(mu(3)-pyridine-2,4-dicarboxylato-kappa N-4,O-1:O-1 ':O-4)dicerium(III)] monohydrate]. *Acta Crystallogr E* **2012**, *68*, M21-+.
48. Silveira, C. C.; Mendes, S. R.; Ziembowicz, F. I.; Lenardao, E. J.; Perin, G., The Use of Anhydrous CeCl3 as a Recyclable and Selective Catalyst for the Acetalization of Aldehydes and Ketones. *J Brazil Chem Soc* **2010**, *21*, 371-374.
49. Cao, C. C.; Chen, C. X.; Wei, Z. W.; Qiu, Q. F.; Zhu, N. X.; Xiong, Y. Y.; Jiang, J. J.; Wang, D. W.; Su, C. Y., Catalysis through Dynamic Spacer Installation of Multivariate Functionalities in Metal-Organic Frameworks. *J Am Chem Soc* **2019**, *141*, 2589-2593.
50. Talebian-Kiakalaieh, A.; Amin, N. A. S.; Najaafi, N.; Tarighi, S., A Review on the Catalytic Acetalization of Bio-renewable Glycerol to Fuel Additives. *Front Chem* **2018**, *6*.
51. Kanai, S.; Nagahara, I.; Kita, Y.; Kamata, K.; Hara, M., A bifunctional cerium phosphate catalyst for chemoselective acetalization. *Chem Sci* **2017**, *8*, 3146-3153.

For Table of Contents Use Only

Ce(III)-based Frameworks: From 1D Chain to 3D Porous Metal-Organic Framework

Parviz Gohari Derakhshandeh[*a,b†], Sara Abednatanzi[a†], Karen Leus[a] , Jan Janczak[c], Rik Van Deun[d], Pascal Van Der Voort[a], Kristof Van Hecke[*b]

Three new 1D, 2D and 3D Ce(III)-based frameworks were developed by small changes in the synthetic routs. Lanthanide ions are outstanding candidates to adopt distinct coordination environments due to their adjustable coordination modes which is an important step towards the engineering of Ln-based frameworks for more specialized applications.